JACS
JOURNAL OF THE AMERICAN CHEMICAL SOCIETY

Communication

pubs.acs.org/JACS

Deconstructing Activation Events in Rhodopsin

Elena N. Laricheva,[†] Karunesh Arora,[†] Jennifer L. Knight,[§] and Charles L. Brooks, III*[,†,‡]

[†]Department of Chemistry and [‡]Biophysics Program, University of Michigan, Ann Arbor, Michigan 48109, United States

Supporting Information

ABSTRACT: Activation of class-A G-protein-coupled receptors (GPCRs) involves large-scale reorganization of the H3/H6 interhelical network. In rhodopsin (Rh), this process is coupled to a change in the protonation state of a key residue, E134, whose exact role in activation is not well understood. Capturing this millisecond pH-dependent process is a well-appreciated challenge. We have developed a scheme combining the harmonic Fourier beads (HFB) method and constant-pH molecular dynamics with pH-based replica exchange (pH-REX) to gain insight into the structural changes that occur along the activation pathway as a function of the protonation state of E134. Our results indicate that E134 is protonated as a consequence of tilting of H6 by ca. 4.0° with respect to its initial position and simultaneous rotation by ca. 23° along its principal axis. The movement of H6 is associated with breakage of the E247−R135 and R135−E134 salt bridges and concomitant release of the E134 side chain, which results in an increase in its pK_a value above physiological pH. An increase in the hydrophobicity of the environment surrounding E134 leads to further tilting and rotation of H6 and upshift of the E134 pK_a. Such atomic-level information, which is not accessible through experiments, refines the earlier proposed sequential model of Rh activation (see: Zaitseva, E.; et al. Sequential Rearrangement of Interhelical Networks Upon Rhodopsin Activation in Membranes: The Meta II$_a$ Conformational Substate. *J. Am. Chem. Soc.* **2010**, *132*, 4815) and argues that the E134 protonation switch is both a cause and a consequence of the H6 motion.

A hallmark of the transition between inactive and active forms of heptahelical G-protein-coupled receptors (GPCRs) is the large (3−14 Å) outward tilt of transmembrane helix 6 (H6) in response to various extracellular stimuli, such as light or ligand binding.[1,2] This tilt causes rearrangements in the H3/H6 interhelical network and creates a cavity for the binding of the heterotrimeric G-protein, thus initiating a cascade of signaling events inside a cell.[3] In rhodopsin (Rh), the most widely studied class-A GPCR, there are several pre- and postrequisites for the H6 motion, including a series of conformational and protonation switches in the late stages of activation.[4,5] Following ultrafast 11-*cis* to all-*trans* photoisomerization[6] of the retinal protonated Schiff base (11-PSB), formed by covalent binding of the chromophore retinal to K296, the signal is propagated from the dark state through a series of inactive intermediates to a cytoplasmic receptor domain, where a signaling Meta II state capable of binding the G-protein is formed (Figure 1A).[3,7]

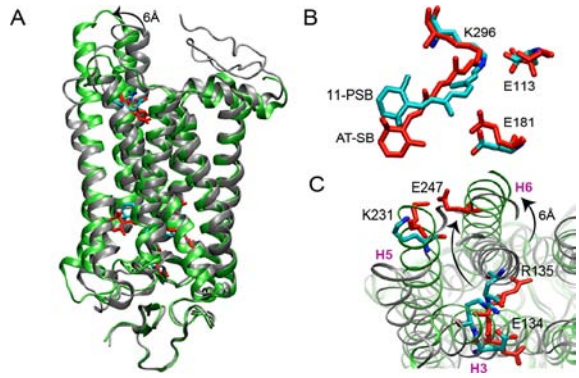

Figure 1. (A) Dark (gray and cyan) and Meta II (green and red) states of Rh. (B, C) Regions involved in the two protonation-dependent switches.

While early transitions can be exclusively described by the small-scale rearrangements in the retinal binding pocket needed to accommodate the isomerized chromophore,[8] the major functional and structural changes of the α-helical bundle occur during the pH-dependent Meta I to Meta II transition.[9,10] According to the activation scheme originally proposed by Hofmann, Hubbell, and colleagues[11,12] and later corroborated and extended by Vogel and co-workers,[13,14] this transformation occurs sequentially via the series of metastable states Meta II$_a$, Meta II$_b$, and Meta II$_b$-H$^+$, with the latter two collectively representing the Meta II form. In this scheme, Meta II$_a$ is formed upon disruption of the salt bridge between the all-*trans* protonated Schiff base (AT-PSB) and the primary counterion E113 via an internal proton transfer between the two moieties with the formation of an unprotonated Schiff base (AT-SB) (the first protonation switch; Figure 1B); Meta II$_b$ stems from the 6 Å outward tilt of H6; and Meta II$_b$-H$^+$ is a result of proton uptake by E134 of the conserved E(D)RY motif located on H3 near the cytoplasmic water−lipid interface (the second protonation switch; Figure 1C). Although the suggested reaction scheme is supported by a number of experimental studies,[9,11,12,14] a precise dynamical picture of how the proposed structural changes occur is still missing. Molecular dynamics (MD) simulations can provide a detailed answer to this question and thus have been widely exploited by different research groups.[15] However, capturing this millisecond

Received: May 9, 2013
Published: July 10, 2013

   dx.doi.org/10.1021/ja4042687 | *J. Am. Chem. Soc.* 2013, 135, 10906−10909

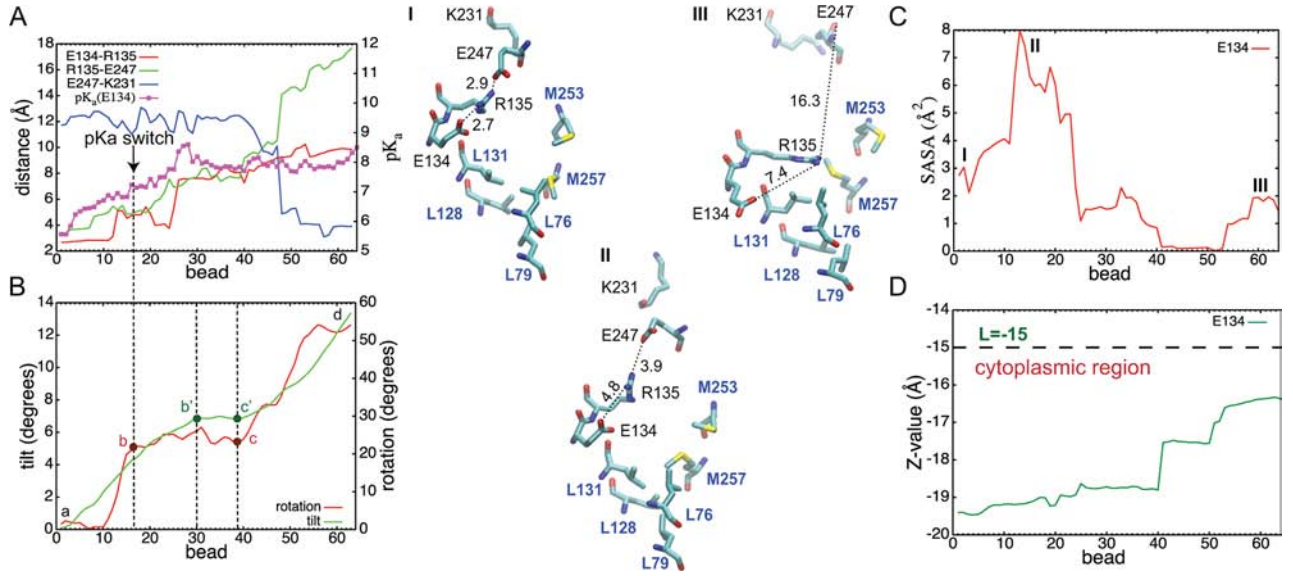

Figure 2. Values computed along the Meta II_a to Meta II pathway: (A) pK_a of E134 and average salt bridge distances measured between the closest oxygens and nitrogens of the corresponding acidic (E134, E247) and basic (R135, K231) residues; (B) H6 tilt and rotation angles; (C) SASA of the E134 side chain; (D) *Z* value showing the position of the E134 center of mass relative to the center of the lipid bilayer. Changes in the E(D)RY motif with respect to a hydrophobic barrier at different points of the pathway are shown for the end states (I and II) and in the region of the pK_a switch (III).

transition is beyond the reach of standard MD simulations. Several attempts have been made to overcome the time scale limitation and to arrive at the Meta II state by running long MD simulations guided by the NMR distance restraints starting from either the dark state[16] or, most recently, from lumirhodopsin.[17] These calculations, however, all assumed fixed protonation states during the dynamics and did not consider on-the-fly coupling between pH and conformational switching, as we have done in the current work. Here, we have delineated a sequence of late activation events in Rh by probing a conformational transition between its putative semiactive Meta II_a and active Meta II forms as a function of the protonation state of E134.

We used the 4.15 Å (PDB entry 2I37) and 3.0 Å (3PXO) X-ray structures to construct initial models of the Meta II_a and Meta II states, respectively. We utilized the generalized Born with simple switching (GBSW)[18,19] implicit solvent/implicit membrane model to determine an optimal position of each structure in the membrane and used the corresponding lowest-energy configurations as the starting points to generate a transition pathway between the initial Meta II_a and final Meta II states using the harmonic Fourier beads method (HFB).[20] Prior to generation of the pathway, constant-pH molecular dynamics[21] with pH-based replica exchange (pH-REX)[22] was used to determine the protonation states of E113, E181, and E134 in the starting Meta II_a and final Meta II states. E113 and E181 were found to be protonated in both states, so these residues were modeled as neutral in all subsequent simulations. Once the path was generated, pH-REX was used to capture the protonation state of E134 along the conformational transition pathway. All of the calculations were performed using the CMAP-corrected[23] all-atom CHARMM22 force field for proteins.[24] For details of the computational methods and analysis, see the Supporting Information (SI).

Our results show that the pK_a of E134 changes from 5.6 to 8.3 during the transition, with a protonation switch (pK_a = 7.4) occurring early along the computed path (Figure 2A). This process is associated with breakage of the E134−R135 and R135−E247 salt bridges that hold Rh in the semiactive conformation and subsequent formation of the new E247−K231 ionic lock that stabilizes the Meta II state. The R135−E247 salt bridge breaks first, releasing the side chain of E134 and allowing its pK_a to rise, as confirmed by the pK_a switch to 7.4 shortly afterward. The outward tilt of H6, as monitored using the angle between the helical axis at a given point of the pathway and the initial axis position, is depicted in Figure 2B. The observed tilt is sequential (segments $a-b'$, $b'-c'$, and $c'-d$; green line) and is partially coupled to the rotation of H6 along its principal axis, which also occurs in a sequential manner (segments $a-b$, $b-c$, and $c-d$; red line). As shown, the E134 protonation switch associated with breakage of the R135−E247 and E134−R135 salt bridges, is a consequence of rotation of H6 by ca. 23° along the helical axis (segment $a-b$) with a simultaneous outward tilt by ca. 4°. Later (region $b-c$), the H6 tilt and rotation are partially decoupled, with H6 continuing to tilt but not rotating anymore, while their coupled motion becomes apparent again along the $c-d$ and $c'-d$ segments. The latter changes, characterized by an additional helical rotation of ca. 30° and an outward tilt of ca. 10° that bring the H5 and H6 extracellular ends together, accompany the shift of the pK_a of E134 from 7.4 to 8.3.

Our results are in apparent disagreement with the experimental interpretation suggesting that proton uptake by E134 in Rh does not happen unless H6 has fully moved.[12−14] These experimental conclusions are based on the observed pH independence of the electron paramagnetic resonance (EPR) signal arising from immobilization of the nitroxide side chain in the spin-labeled V227C Rh mutant (R227) in response to the outward tilt of H6.[12] In this mutant, R227 belongs to the neighboring helix H5 and senses the changes in the surrounding environment. Once the outward tilt of H6 in the direction of H5 becomes sufficiently large, the spin label can sense the change in the environment, giving rise to the EPR signal. Since the maximum amplitude of the EPR signal

dx.doi.org/10.1021/ja4042687 | J. Am. Chem. Soc. 2013, 135, 10906−10909

remained the same over the entire pH range from 5 to 9, it was concluded that the E134 proton uptake followed the H6 motion. On the basis of our results, we provide an alternative explanation of the observed pH independence of the EPR signal. Along segment $a-b'$, an outward tilt of H6 is expected to be strongly pH-dependent due to the large shift of the pK_a of E134 from 5.6 to 7.4, but the small tilt angle (ca. 4°) associated with it is insufficient to cause the immobilization of the spin label and saturation of the EPR signal. The latter conclusion is confirmed by the small number of contacts that R227 makes with H6 along that portion of pathway (Figure S7 in the SI). In contrast, along segment $b'-d$, which is associated with an easily detectable H6 tilt (ca. 10°), the pK_a shift is significantly smaller (7.4 to 8.3) and the expected pH dependence of the tilt is small as well. Accordingly, the computed number of contacts along $b'-d$ substantially increases, as depicted in Figure S7. Thus, our results call for the reinterpretation of the EPR data on Rh and reconsideration of the existing activation scheme.

To understand the origin of the pK_a shift, the solvent-accessible surface area (SASA) of E134 was computed along the transition pathway (Figure 2C). It increases up to the point where the E134 protonation switch occurs, in agreement with the observed breakage of the E247−R135 and E134−R135 salt bridges that release the side chain of E134, exposing it to the solvent. Then, along the portion of the pathway corresponding to the shift of the pK_a from 7.4 to 8.3, the SASA gradually drops, indicating an increase in hydrophobicity of the environment surrounding the side chain of E134. As Figure 2D illustrates, this is in part due to a desolvation effect and displacement of the side chain from the water bulk closer to the lipid−water interface (from $L = -19.4$ to $L = -17.5$, where $L = -15$ indicates a position of the lower membrane plane lying on the cytoplasmic side of the 30 Å thick implicit lipid bilayer used in our study.)

Another important factor that contributes to the pK_a shift is the exposure of the E134 side chain to the so-called "hydrophobic barrier",[25] consisting of L76, L79, L128, L131, M253, and M257. Structural rearrangements of the E(D)RY motif with respect to this region along the Meta II_a to Meta II transition pathway are shown in Figure 2 (structures I−III). Upon breakage of the E247−R135 and E134−R135 salt bridges preceding the E134 protonation switch, the released E134 side chain makes close contacts with L128 and L131 and becomes deeply buried inside the protein. The more hydrophobic environment stabilizes the neutral form of E134 and leads to a shift of its pK_a from 7.4 to 8.3. Notably, no experimental data on the pK_a values of the ionizable residues in Rh exist. However, our predictions agree well with the change in the E134 protonation state determined experimentally[26,27] as well as with the electrostatic MM-SCP calculations by Periole et al.[28] It is also worth noting that constant-pH MD calculations based on the GBSW implicit solvent model have been successfully applied to many proteins[29−32] where comparison between experimental and computed values could be rigorously made, yielding a root-mean-square error of 0.6 pH units for proteins containing few buried ionizable side chains.[29] On the basis of the precision of the pK_a values in our simulations, the shift in pK_a from 7.4 to 8.3 that we observe is statistically significant at the 95% confidence interval, so the observed change reflects conformational dynamics of the protein and allows us to delineate a sequence of activation events using the protonation state of E134 as a reaction coordinate.

Overall, the results of our study combining the HFB method and pH-REX simulations have enabled us to derive a detailed mechanistic picture of the late activation events in Rh and elucidate mechanistic details of the coupling between the change in the protonation state of E134 and the conformational dynamics of the protein. HFB made it possible to explore the reaction pathway without making any prior assumptions about the reaction mechanism, and performing pH-REX at every point of the pathway allowed us to incorporate the information about the protonation state of E134 on the fly and thus probe the existing sequential Meta II_a−Meta II_b−Meta II_b-H^+ reaction scheme.[10−12] While the experimental data suggest that proton uptake by E134 is a consequence of H6 motion, our simulations offer an alternative explanation. We have shown that E134 is protonated early along the computed path as a consequence of tilting of H6 by ca. 4.0° with respect to the membrane normal and simultaneous rotation by ca. 23° along the helical axis. This process is associated with breakage of the E247−R135 and R135−E134 salt bridges, releasing the side chain of E134 and allowing its pK_a to increase to a value above physiological pH. This in turn leads to a further ca. 10° tilt and ca. 30° rotation of H6 together with a 2−3 Å translation of the E134 side chain toward the center of the membrane, causing the additional upshift of its pK_a. In the first segment of the pathway, the expected pH dependence of the H6 tilt (associated with the significant change in the pK_a of E134 from 5.6 to 7.4) is large, but we argue that the small value of the tilt is insufficient to cause immobilization of the spin label in the EPR experiment and saturate the EPR signal. In the second region, however, the tilt is large enough to be observed, but the expected pH dependence of the tilt is negligible because of the 2-fold smaller modulation of the pK_a.

■ ASSOCIATED CONTENT

Ⓢ Supporting Information

Details of the computational protocol and analysis. This material is available free of charge via the Internet at http://pubs.acs.org.

■ AUTHOR INFORMATION

Corresponding Author

brookscl@umich.edu

Present Address

[§]Schrodinger, Inc., 120 West 45th Street, New York, New York 10036, United States.

Notes

The authors declare no competing financial interest.

■ ACKNOWLEDGMENTS

This work was supported by the NIH (GM037554 and GM057513).

■ REFERENCES

(1) Venkatakrishnan, A. J.; Deupi, X.; Lebon, G.; Tate, C. G.; Schertler, G. F.; Babu, M. M. *Nature* **2013**, *494*, 185−194.

(2) Deupi, X.; Standfuss, J. *Curr. Opin. Struct. Biol.* **2011**, *21*, 541−551.

(3) Hubbell, W. L.; Altenbach, C.; Hubbell, C. M.; Khorana, H. G. *Adv. Protein Chem.* **2003**, *63*, 243−290.

(4) Trzaskowski, B.; Latek, D. *Curr. Med. Chem.* **2012**, *19*, 1090−1109.

(5) Vogel, R.; Mahalingam, M.; Ludeke, S.; Huber, T.; Siebert, F.; Sakmar, T. P. *J. Mol. Biol.* **2008**, *380*, 648−655.

(6) Schoenlein, R. W.; Peteanu, L. A.; Mathies, R. A.; Shank, C. V. *Science* **1991**, *254*, 412−415.
(7) Choe, H.; Kim, Y.; Park, J.; Morizumi, T. *Nature* **2011**, *471*, 651−655.
(8) Struts, A. V.; Salgado, G. F. J.; Tanaka, K.; Krane, S.; Nakanishi, K.; Brown, M. F. *J. Mol. Biol.* **2007**, *372*, 50−66.
(9) Altenbach, C.; Kusnetzow, A. *Proc. Natl. Acad. Sci. U.S.A.* **2008**, *105*, 7439−7444.
(10) Farrens, D. L.; Altenbach, C.; Yang, K.; Hubbell, W. L.; Khorana, H. G. *Science* **1996**, *274*, 768−770.
(11) Arnis, S.; Hofmann, K. P. *Proc. Natl. Acad. Sci. U.S.A.* **1993**, *90*, 7849−7853.
(12) Knierim, B.; Hofmann, K. P.; Ernst, O. P.; Hubbell, W. L. *Proc. Natl. Acad. Sci. U.S.A.* **2007**, *104*, 20290−20295.
(13) Mahalingam, M.; Martínez-Mayorga, K.; Brown, M. F.; Vogel, R. *Proc. Natl. Acad. Sci. U.S.A.* **2008**, *105*, 17795−17800.
(14) Zaitseva, E.; Brown, M. F.; Vogel, R. *J. Am. Chem. Soc.* **2010**, *132*, 4815−4821.
(15) Grossfield, A. *Biochim. Biophys. Acta* **2011**, *1808*, 1868−1878.
(16) Hornak, V.; Ahuja, S.; Eilers, M. *J. Mol. Biol.* **2010**, *396*, 510−527.
(17) Tikhonova, I.; Best, R. *J. Am. Chem. Soc.* **2008**, *130*, 10141−10149.
(18) Chen, J.; Im, W.; Brooks, C. L., III. *J. Am. Chem. Soc.* **2006**, *128*, 3728−3736.
(19) Im, W.; Feig, M.; Brooks, C. L., III. *Biophys. J.* **2003**, *85*, 2900−2918.
(20) Khavrutskii, I. V.; Arora, K.; Brooks, C. L., III. *J. Chem. Phys.* **2006**, *125*, No. 174108.
(21) Khandogin, J.; Brooks, C. L., III. *Biophys. J.* **2005**, *89*, 141−157.
(22) Sugita, Y.; Okamoto, Y. *Chem. Phys. Lett.* **1999**, *314*, 141−151.
(23) Mackerell, A. D., Jr.; Feig, M.; Brooks, C. L., III. *J. Comput. Chem.* **2004**, *25*, 1400−1415.
(24) MacKerell, A. D., Jr.; Bashford, D.; Bellott, M.; Dunbrack, R. L., Jr.; Evanseck, J. D.; Field, M. J.; Fischer, S.; Gao, J.; Guo, H.; Ha, S.; Joseph-McCarthy, D.; Kuchnir, L.; Kuczera, K.; Lau, F. T. K.; Mattos, C.; Michnick, S.; Ngo, T.; Nguyen, D. T.; Prodhom, B.; Reiher, W. E., III; Roux, B.; Schlenkrich, M.; Smith, J. C.; Stote, R.; Straub, J.; Watanabe, M.; Wiórkiewicz-Kuczera, J.; Yin, D.; Karplus, M. *J. Phys. Chem. B* **1998**, *102*, 3586−3616.
(25) Standfuss, J.; Edwards, P. C.; D'Antona, A.; Fransen, M.; Xie, G.; Oprian, D. D.; Schertler, G. F. X. *Nature* **2011**, *471*, 656−660.
(26) Yan, E. C. Y.; Kazmi, M. A.; Ganim, Z.; Hou, J.-M.; Pan, D.; Chang, B. S. W.; Sakmar, T. P.; Mathies, R. A. *Proc. Natl. Acad. Sci. U.S.A.* **2003**, *100*, 9262−9267.
(27) Fahmy, K.; Sakmar, T. P.; Siebert, F. *Biochemistry* **2000**, *39*, 10607−10612.
(28) Periole, X.; Ceruso, M.; Mehler, E. *Biochemistry* **2004**, *43*, 6858−6864.
(29) Khandogin, J.; Brooks, C. L., III. *Biochemistry* **2006**, *45*, 9363−9373.
(30) Khandogin, J.; Chen, J.; Brooks, C. L., III. *Proc. Natl. Acad. Sci. U.S.A.* **2006**, *103*, 18546−18550.
(31) Zhang, B. W.; Brunetti, L.; Brooks, C. L., III. *J. Am. Chem. Soc.* **2011**, *133*, 19393−19398.
(32) Law, S. M.; Zhang, B. W.; Brooks, C. L., III. *Protein Sci.* **2013**, *22*, 595−604.